R
385
5-23-61

IDO-16617

MASTER

QUARTERLY TECHNICAL REPORT
SPERT PROJECT
January, February, March, 1960

T. R. Wilson, Ed.

March 31, 1961

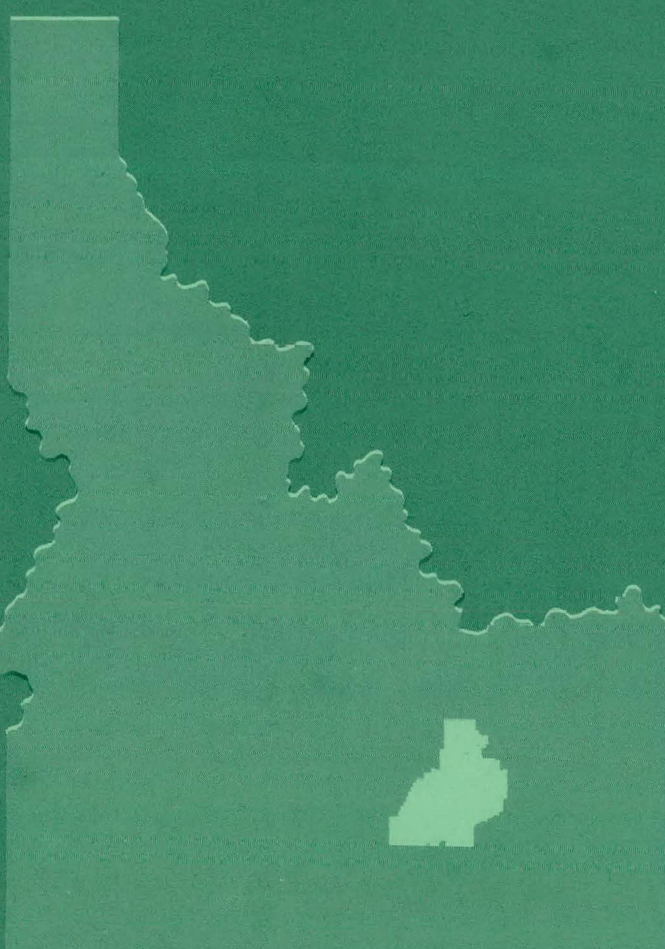

PHILLIPS
PETROLEUM
COMPANY

ATOMIC ENERGY DIVISION

NATIONAL REACTOR TESTING STATION
US ATOMIC ENERGY COMMISSION

DISCLAIMER

PRICE $ .75

Available from the
Office of Technical Services
U. S. Department of Commerce
Washington 25, D. C.

Printed in USA

IDO-16617
AEC Research and Development Report
Reactor Technology
TID-4500 (16th Ed.)

QUARTERLY TECHNICAL REPORT
SPERT PROJECT

January, February, March, 1960

T. R. Wilson, ed.

APPROVED:

J. R. Huffman
Assistant Manager, Technical

W. E. Nyer
Manager, Reactor Projects Branch

PHILLIPS PETROLEUM COMPANY
Atomic Energy Division
Idaho Falls, Idaho
Contract AT(10-1)-205

IDAHO OPERATIONS OFFICE
U. S. Atomic Energy Commission

Previous Quarterly Reports

Spert Project

1957

Quarter	Report No.
3	IDO-16416
4	IDO-16437

1958

Quarter	Report No.
1	IDO-16452
2	IDO-16489
3	IDO-16512
4	IDO-16537

1959

Quarter	Report No.
1	IDO-16539
2	IDO-16584
3	IDO-16606
4	IDO-16616

TABLE OF CONTENTS

TABLE

LIST OF FIGURES

I. SUMMARY

SPERT I - A series of experiments relating to the problem of reactor startup from very low initial power has been performed with a cold, clean, stainless steel core in the Spert I facility. The intrinsic neutron source level for this core was measured and found to be approximately 500 n/sec. Time delays were observed between the step-wise injection of reactivity at power levels of about 10^{-5} watts and the attainment of a stable period. In some cases these delays, which are attributed in part to the statistical properties of neutron chains, were as long as 2 seconds. In one sourceless startup test, control rods were withdrawn at a rate of 20¢/sec with period and level scram circuits operative. The period circuit scrammed the reactor at a trivial power level before the reactor period became shorter than 50 msec.

SPERT II - Construction of the Spert II facility was completed February 1, 1960. Initial criticality was achieved in light water with 24, type "B" fuel assemblies containing 24 plates each and 8, 17-plate, control rod assemblies. The total U-235 mass of this initial core was 4.69 kg. On the basis of differential rod worth data, the critical mass for this configuration was estimated to be 4.6 kg of U-235. An operational core loading containing 6.03 kg of U-235 was found to have an available excess reactivity of about \$2 at a temperature of 400°F and about \$6.8 at ambient temperature.

In anticipation of future transient testing of a core with a central positive void coefficient, a core loading was investigated in which the plate spacing was increased for the central fuel assemblies. The central void coefficient of approximately + 2 x 10^{-2} ¢/cm^3 was measured for this core.

SPERT III - In order to obtain power calibration data for the Spert III neutron chambers and to provide information for future use in the analysis of transient data, the neutron flux distribution has been measured at ambient temperature in the Spert III operational core by activation of cobalt wires. The average power level during the irradiation was calculated from the measured flux values and combined with the neutron chamber output data to yield approximate calibration factors for each chamber. The results indicate that power levels from 5 w to 20 Gw can be measured with the present arrangement of four chambers.

ENGINEERING - The hydraulic characteristics of the type "D" fuel assemblies have been investigated. These loose-plate-type assemblies have been designed for use in the Spert IV reactor. The pressure drop as a function of flow was calculated and found to agree very well with the experimental data obtained in the ETR flow test loop. Plate flutter is not excessive with flow rates up to 610 gpm through the assembly and it is concluded that the type "D" assembly will be acceptable hydrodynamically for use in Spert IV.

Pressure-flow relationships have been calculated as a function of water temperature for type "B" fuel assemblies with 8, 12, and 24 fuel

plates. The calculations agree with available experimental data at 85°F for the 24-plate assembly.

II. SPERT I

A. Low-Level Startup (F. L. Bentzen)

A series of experiments relating to a basic safety problem of reactor startup or runaway from very low initial power has been performed with the Bulk Shielding Reactor (BSR-II) stainless steel core in the Spert I facility.(1) In these experiments, the intrinsic neutron source level was measured, the delay in initiating a sustaining fission chain was determined for a series of step transients and a sourceless startup test was performed in which the control rods were withdrawn at the maximum rate available.

The general problem of concern in these experiments arises from the possibility that the reactivity added to the system during startup from a very low source level might significantly exceed safe limits before the power level is great enough for inherent reactivity compensating mechanisms to be effective or before detectable signals appear. The problem is a consequence of the low neutron population in the system and the statistical nature of fission chains. Usually an artificial neutron source of sufficient magnitude is placed in the core to obviate these problems. The source insures that a sufficient number of neutrons is available to immediately start a continuing neutron chain and provides the signal required by the operator or control system. Information related to the source problem was obtained in the experiments described below.

1. Inherent Neutron Source Level

The inherent source level in the cold BSR-II core was determined by comparing the neutron counting rate at multiplications of approximately 10, 250, and 500, both with and without a Ra-Be source of 1.5×10^3 n/sec in the core. Although the relative importance of the point source as compared with the inherent distributed source was not taken into account in this rather elementary experiment, the values obtained--370, 540, and 410 n/sec--indicate that a value of 500 n/sec can be used as a reasonable approximation for the inherent source level.

2. Statistical Delay Times

Certain of the power excursion tests, performed with the BSR-II core, required starting powers in the milliwatt region. An artificial neutron source was not used and the neutron level in the reactor was allowed to decay to a very low value prior to the initiation of the excursion. The estimated starting power level was 10^{-5} w but was not necessarily identical for all the tests. Measurements were made of the elapsed time between the seating of the transient rod, which initiated the power excursion, and the attainment of a 100 kw power level. The time required for the reactor power to rise on the measured asymptotic period from the estimated starting power level to 100 kw was calculated and subtracted from the observed elapsed time.

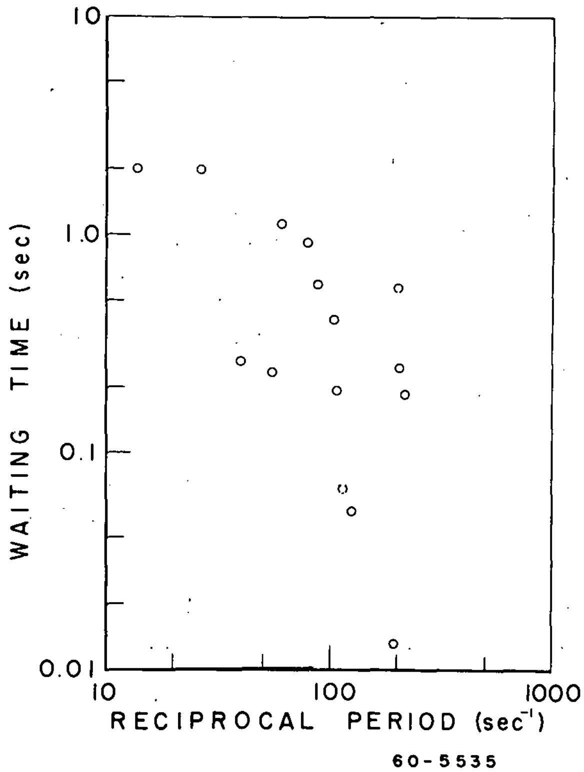

Fig. 1 - Estimated Waiting Time for Attainment of Stable Reactor Period Versus Reciprocal Period

Negative values of the difference indicated that the power rise had been initiated before the rod was seated. Positive values indicated the possible existence of a delay time in the initiation of the power rise. The positive values are denoted "waiting time" and are shown in Fig. 1 as a function of reciprocal period. While the complexity of the statistical problem prevents this waiting time from being identified as the delay time in initiating a continuing chain, the waiting time can be used as the effective time during which unwanted reactivity could be added to the system.

The scatter in the data is due in part to the statistical nature of the delay, uncertainties in the actual starting power, and the calculational approach. It is evident from the data that in some tests considerable time delays did exist between the injection of reactivity and the attainment of a stable period. The waiting time as defined above and the rate of reactivity injection are determining factors in the potential hazards of reactor operation at very low power levels.

3. Blind and Sourceless Startup Test

Rapid withdrawal of control rods from a cold reactor with no artificial source present and no indication of neutron level is generally considered to be a dangerous or at least an unwise procedure to follow. Further consideration indicates that this is not necessarily true. But since such a procedure may constitute a potential accident for many reactor systems, a single test following these procedures was performed on the BSR-II core in Spert I with all of its safety scram circuits in operation. The level safety was set to scram at 100 kw, the period circuit was set to scram on all periods shorter than 1 sec, and reactivity was inserted at a rate of 20¢/sec which was the maximum available. Under normal conditions this ramp rate would result in a minimum period of 20 msec. A shorter period would be expected if a significant delay in initiation existed. In the one test that was performed, the period circuit scrammed the reactor and the burst was terminated at a trivial power level before the period became shorter than 50 msec.

4. Conclusions

Broad conclusions regarding the operation of an experimental facility without a neutron source cannot be made on the basis of these tests. However, the following specific points are worth noting:

a) After preliminary tests, operation of the reactor was undertaken without an artificial neutron source in the core. Several months of such operation produced no special problems or incidents.

b) The one sourceless, blind startup test that was performed by withdrawal of the control rods at the maximum rate resulted in shutdown by the safety system at a trivial power before the period became shorter than 50 msec.

c) Significant delays can exist between the injection of reactivity and the attainment of a stable period. While such delays are well-known for fast systems such as Godiva[2] the present experiments demonstrate that significant delays can also exist for thermal reactors.

B. BSR-II Safety System (K. E. Krauter)

The reactor safety system utilized during the experiments discussed in the preceding section is described in this section. The system, shown in block diagram form in Fig. 2, is similar to that used at the MTR and many other reactors.

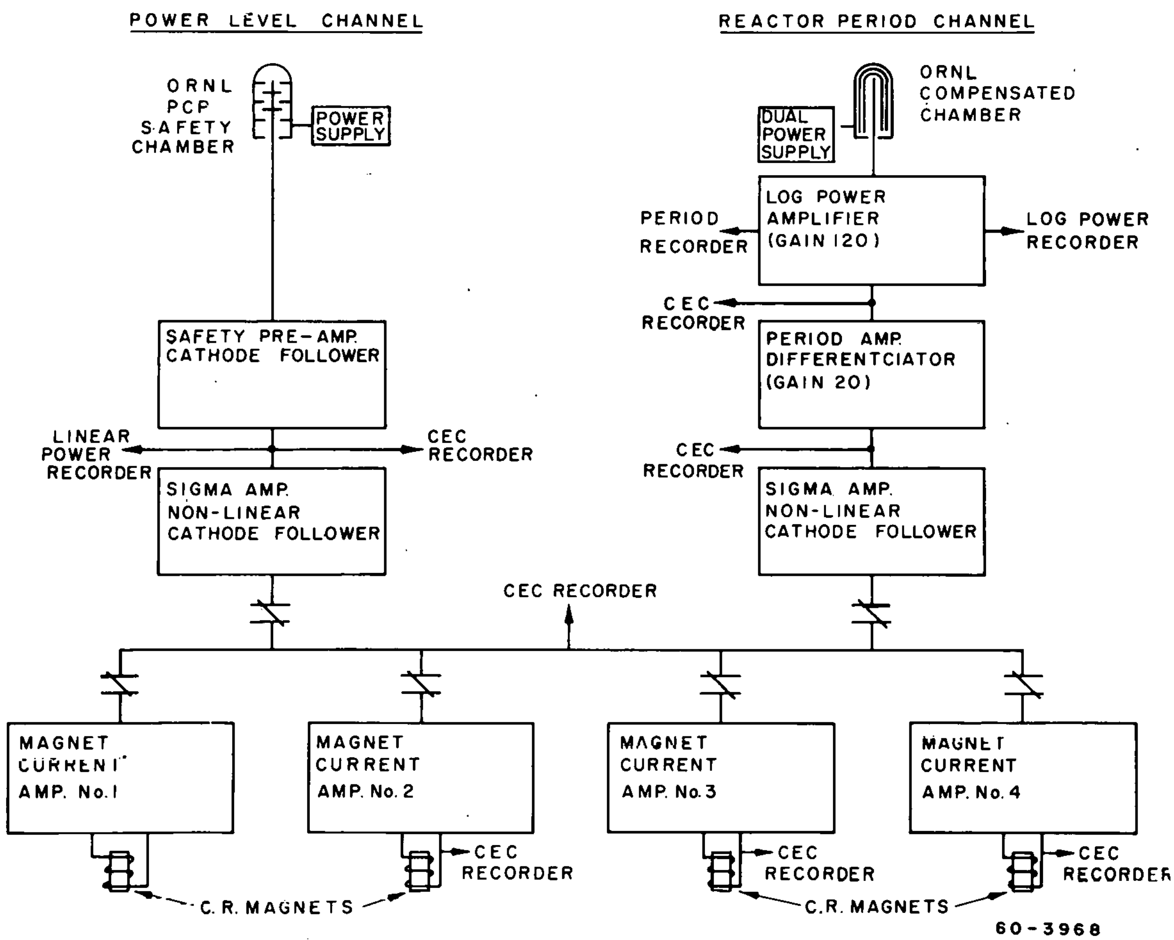

Fig. 2 - BSR-II Safety System for the Spert Installation

The BSR-II safety controls installed for the Spert tests incorporated two reactor power level channels. Each power level scram channel consisted of an ORNL parallel circular plate ion chamber, a safety pre-amplifier, and sigma amplifier. The safety pre-amplifier is a simple cathode follower which presents a very high impedance load to the chamber. The sigma amplifier is a nonlinear cathode follower which drives the sigma bus. The additional power level scram and the period scram all drive the common sigma bus. The sigma bus is normally held at 37 v by the sigma amplifiers. However, when the sigma amplifier voltage rises above 44 v or falls below 33 v the reactor is scrammed by the magnet current amplifiers.

A typical malfunction warning system, as used throughout the safety system, is incorporated in the sigma amplifier. The malfunction system is a current--sensitive relay in the plate of the cathode follower which senses a failure of the power supply, cables not connected, faulty tube filaments and various tube and resistor failures.

The safety system was equipped with strip-chart recorders and a recording oscillograph to record system behavior during the transient tests.

III. SPERT II

A. Preparations for Nuclear Startups (J. E. Grund)

1. Introduction

Construction of the Spert II facility was completed on February 1, 1960. From this date until early March, the installation and checkout of equipment proceeded and various minor plant modifications were undertaken. This section describes those activities which were directly related to the nuclear startup of the reactor using several core configurations.

2. Startup Neutron Source

The startup neutron source was a Ra-Be source with a neutron yield of approximately 2×10^6 n/sec. The source was contained in a double-walled stainless-steel capsule that was mounted in a dummy transient rod. With the source mounted in this manner, it was positioned at the approximate center of the reactor core structure.

3. Reactor Core Coordinate System and Core Designation

The 96 lattice positions in the Spert II reactor have been assigned numbers as shown in Fig. 3. The coordinate system can be described by considering the core to be divided into four quadrants (N, E, S, and W) by the cross. Numbers are assigned to each lattice position by considering each quadrant separately as the first quadrant of a normal cartesian coordinate system with the origin at the center of the core. A given position is designated by quadrant, and by X- and Y- coordinates within the quadrant; e.g., W4-2. Thus the fuel-poison control assemblies are located in positions 2-2 and 3-1 in each quadrant and like-numbered positions are symmetric. Control rods are designated by number: Number 1 Control Rod in the North Quadrant, Number 2 in the East Quadrant, etc.

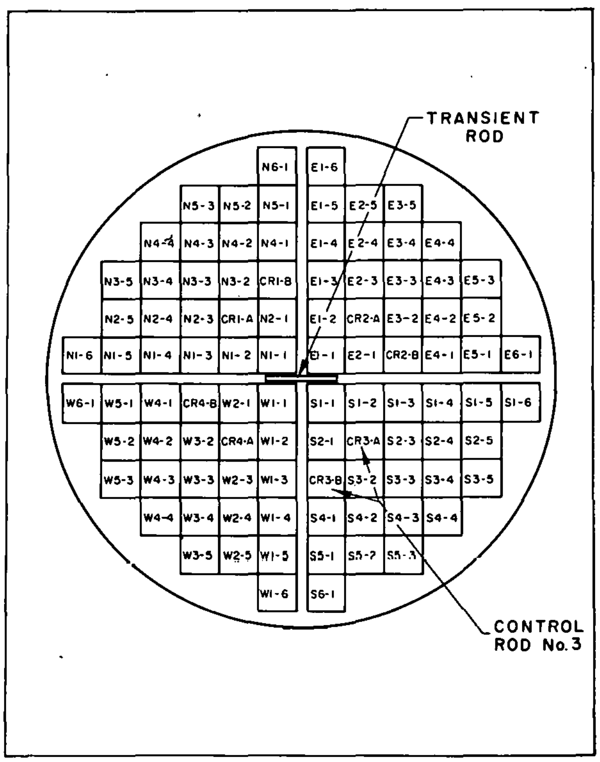

60-3385

Fig. 3 - Spert II Core Coordinate System

The fuel assemblies are referred to as B-24, B-8, etc. This indicates that they are Spert type B fuel assemblies[3] with 24, 8 or other designated number of fuel plates per assembly. The control rods have a similar notation to that of the fuel assemblies, i.e., CR-17, CR-8, which indicates the number of fuel plates in the fuel section of the rod.

4. Instrumentation for Nuclear Startup

The instrumentation used in the startup of Spert II consisted of five neutron pulse-counting systems and two compensated ion chambers.

Each pulse system consisted of a B^{10}-lined chamber and associated pre-amplifiers, power supplies, linear amplifier and scaler. There were two pulse chambers per scaler, Fig. 4, the chambers being selected individually by a switch on the control room nuclear console. Prior to startup of the reactor, each pulse-counting system was calibrated to obtain a curve of the counting rate as a function of counter voltage. The chamber was inserted in an aluminum canister and paraffin poured in the space between the canister and the chamber, or the chamber was inserted in a block of paraffin, depending upon the future location of the chamber in the reactor. The canister or paraffin block was then exposed to a Po-Be neutron source. A typical curve of counting rate as a function of voltage is shown in Fig. 5. Once the operating voltage had been selected for the counter, discrimination data were obtained by exposing the chambers separately to the neutron source used above and to an 80 r/hr gamma source. Typical curves are shown in Fig. 6.

The five pulse chambers were placed in the following positions: Chamber 1-A was placed in an aluminum canister, filled with paraffin, and the canister then placed in a modified filler piece in the W4-2 position; chamber 2-B was similarly placed in the W1-6 position; chamber 3-C was placed in a canister and hung in a position 30° west of south, on a bracket just outside the flow skirt; chamber 1-D was placed in a thimble that ran from the outer vessel wall to the flow skirt, the chamber being placed 12 in. from the mouth of this thimble; chamber 2-E was placed 2 ft west of the thimble against the outside of the vessel wall.

All of the chambers were placed so that the sensitive volume of the chamber was on a horizontal plane passing through the center of the reactor. A logarithmic count-rate circuit was provided, with a meter on the reactor control console so that any of the five chamber channels could be monitored.

Two B^{10}-lined compensated ion chambers were also used during the startup to provide log and linear neutron level information at high multiplications and for operation near criticality. The ion chambers were used uncompensated for the nuclear startup. The linear ion chamber was placed inside the thimble as close to the flow skirt as possible in order to give the maximum indication of neutron flux. The log ion chamber was inserted in a paraffin block and hung on a bracket at the mouth of the thimble. Neither of these chambers showed detectable readings when positioned near the reactor vessel with the startup neutron source in the water-filled vessel and all control rods seated. The ion chambers had previously been calibrated for neutron sensitivity and gamma compensation in the MTR thermal column and gamma facility.[4,5]

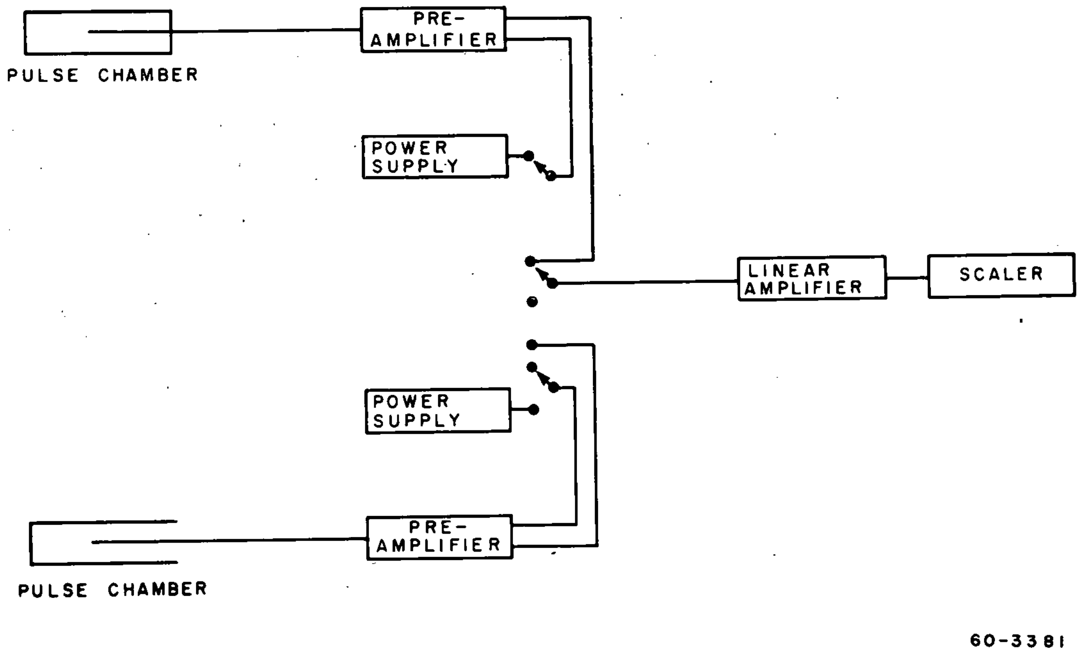

Fig. 4 - Block Diagram of Spert II Startup Instrumentation

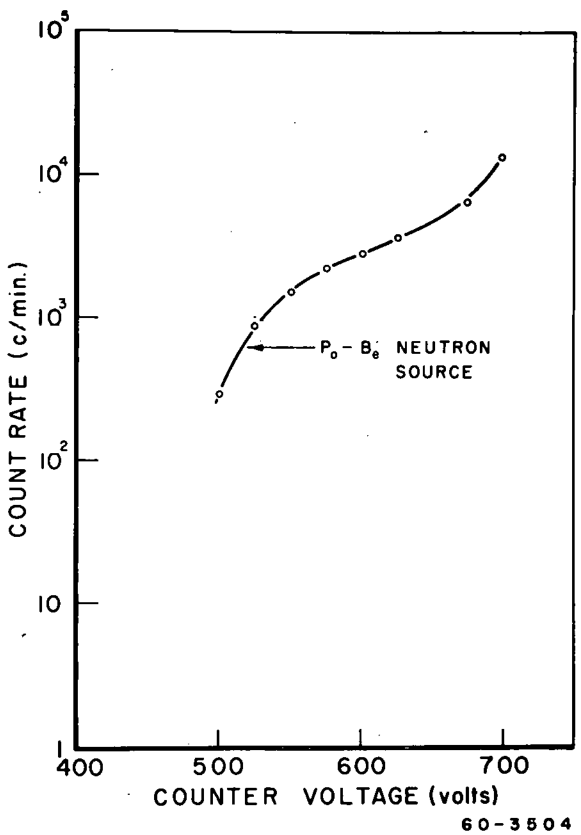

Fig. 5 - Neutron Count Rate vs Counter Voltage for Typical B^{10}-Lined Pulse Counter

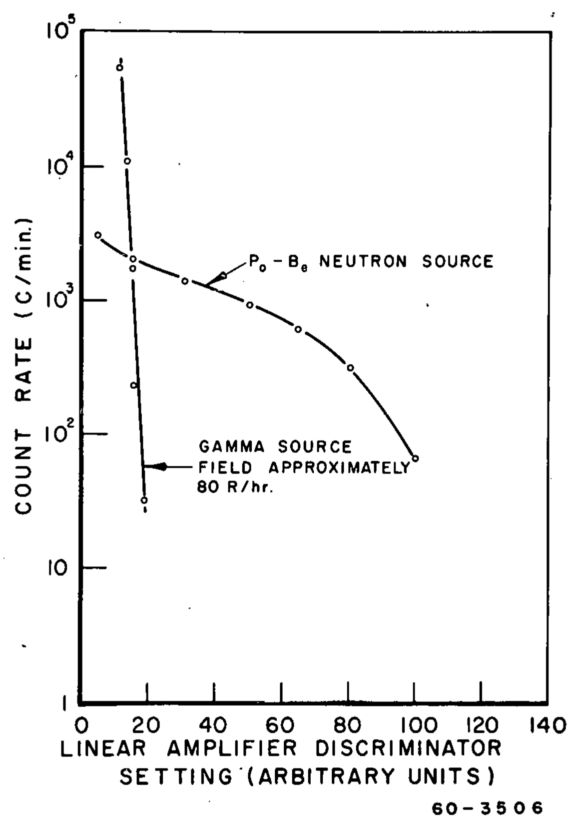

Fig. 6 - Neutron and Gamma Ray Discriminator Curves for Typical B^{10}-Lined Pulse Counter

B. Spert II Startup with the 24-Plate "B" Core (J. G. Crocker)

The initial loading of a critical configuration in the Spert II reactor was accomplished using "B" type assemblies fully loaded with 24 plates each and eight 17-plate fuel-poison control rods. The purpose of the initial experiments was to find the minimum critical configuration, approximate critical mass, operational configuration, and approximate control rod worth with light water.

The procedure for determining the critical arrangement of this core was, in general, divided into three sequences of operation: fuel loading, data taking and data analysis. The fuel assemblies and fuel plates were those that had previously been used in the Spert I "B" core tests, each plate containing 7 g of U-235, making a fully loaded assembly of 168 g. The fuel section of a typical control rod contained about 81.6 g of U-235 or about 4.8 g per plate. The loading procedure maintained polar symmetry as nearly as possible at all times.

At the completion of each loading, the reproduction factor, k, of the core was determined by comparing the relative neutron flux level, C, for that loading with the relative neutron level with only the Ra-Be neutron source in the core, C_o. The factors, C and C_o, are the average count rates from three counting channels. The reproduction factor was determined from these count rates by use of the following relationships:

$$\frac{C_o}{C} = \frac{1}{M} \quad \text{where M is the multiplication, and } k \cong 1 - \frac{1}{M} .$$

Measurements were made at three rod positions for each loading: 0 in., or just when the fuel sections of the rods start into the core, 12 in., and 24 in., when the fuel sections are exactly mated with the core, in order to obtain information on the control rod worth. A graph of the experimentally determined 1/M values versus mass of U-235 in the core was constructed for each counting channel.

Initial criticality was achieved with the rods at 22.05 in. with the configuration shown in Fig. 7. These 24 fuel assemblies and 8 control rod fuel sections represent a total of 4.69 kg of U-235. The extrapolation of the 24 in. rod position curve predicted a critical mass of about 4.6 kg. This compares with the critical mass of 4.34 kg(3) found in Spert I using the same fuel assemblies but different, blade type control rods.

For the operational core it was deemed necessary to have enough excess reactivity at ambient conditions so that at least two dollars

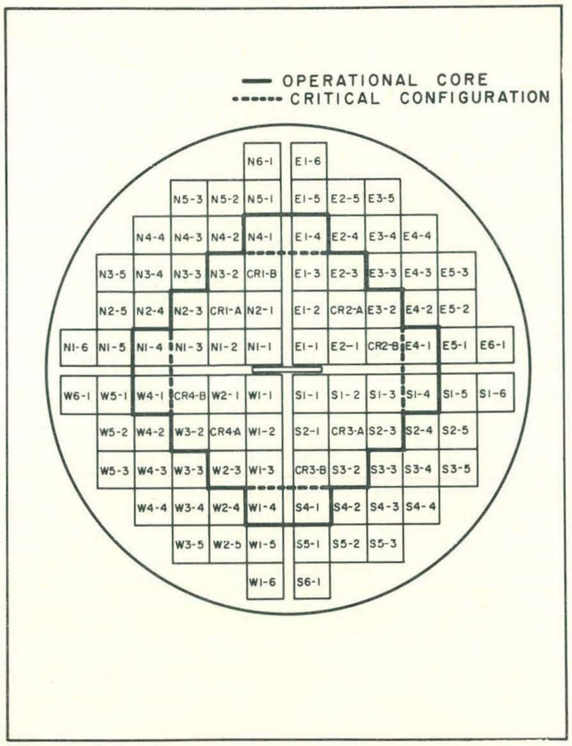

60-3383

Fig. 7 - Spert II 24-Plate Operational Core and Critical Configuration

of excess would be available at maximum conditions of 375 psi and 400°F. The minimum operational core that fit this requirement is also shown in Fig. 7. The total mass of U-235 in the core was 6.03 kg.

The approximate differential worth of the ganged control rods was measured by the period method. The data for several core loadings are given in Table 1. From these data it was determined that the operational core contained approximately 6.8 dollars of excess reactivity at ambient temperature and pressure. Water-filled, aluminum, filler pieces were added to the core to completely fill the grid as would be the case under conditions of flow, temperature, and pressure. By the shift in the critical position it was determined that 35 cents of reactivity was lost due to this addition.

TABLE 1

SUMMARY OF INITIAL PERIOD AND ROD WORTH DATA IN SPERT II 24-PLATE CORE

Run No.	Core	Average Rod Position (in. withdrawn)	Period (sec)	Differential Rod Worth ($/in.)
1	Initial Critical Core	22.10	180	0.35
2	Initial Critical Core	22.16	104	0.32
3	Initial Critical Core	22.26	54	0.31
4	Initial Critical Core plus 3-3 positions	18.15	76	0.81
5	Initial Critical Core plus 3-3 positions	18.19	29	0.85
6	Initial Critical Core plus 4-1 positions	17.25	81	0.92
7	Initial Critical Core plus 4-1 positions	17.30	26	0.97
8	Operational Core	14.45	60	0.37
9	Operational Core	14.47	33.5	0.40

C. "Positive Void Coefficient" Core (J. E. Grund)

A second critical loading was initiated to obtain a "Positive Void Coefficient" Core for the purpose of checking theoretical predictions(6) of the effect of a positive reactivity coefficient on reactor kinetic behavior. The implications of the theory have a bearing on general reactor safety philosophy. For example, the existence and magnitude of a strong negative coefficient of reactivity has been widely used as a measure of reactor safety; however, the theory implies that even this simple requirement should not be used without qualification. The experiments with this core are intended to yield information which will assist in putting the formulation of such general criteria on a sounder basis.

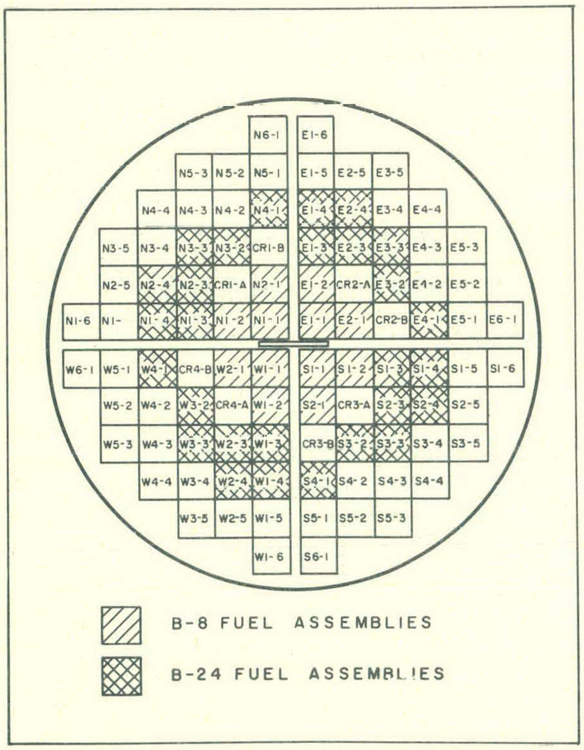

60-3382

Fig. 8 - Initial Spert II Core Configuration for Positive Void Coefficient Core

The general loading procedures for this approach to critical were the same as those followed in the B-24 loading and the instrumentation was identical. The first loading consisted of B-8 assemblies in the central twelve lattice positions, 17-plate control rods, and B-24 assemblies around the periphery of the core. The maximum loading for this approach to critical was 6.04 kg in the configuration shown in Fig. 8. The loading was still subcritical and predictions of the critical mass ranged from 6.5 to 7.4 kg.

It was necessary to go to another variation of this loading as insufficient fuel was available to proceed further. For the variation, the core was loaded with B-8 assemblies in the central four lattice positions. The adjacent eight assemblies were loaded with 16 plates per assembly, such that the plate spacing for the inner half of each was typical of B-8, and the outer half typical of B-24 assemblies as shown in Fig. 9. The remainder of the core was completed with B-24 assemblies. This loading was critical with a total mass of 6.48 kg of U-235 in the core and the control rods at 20.80 in. The extrapolation of the 1/M curve for the 24 in. rod position predicted a critical mass of about 6.3 kg. The final configuration of this core is shown in Fig. 10.

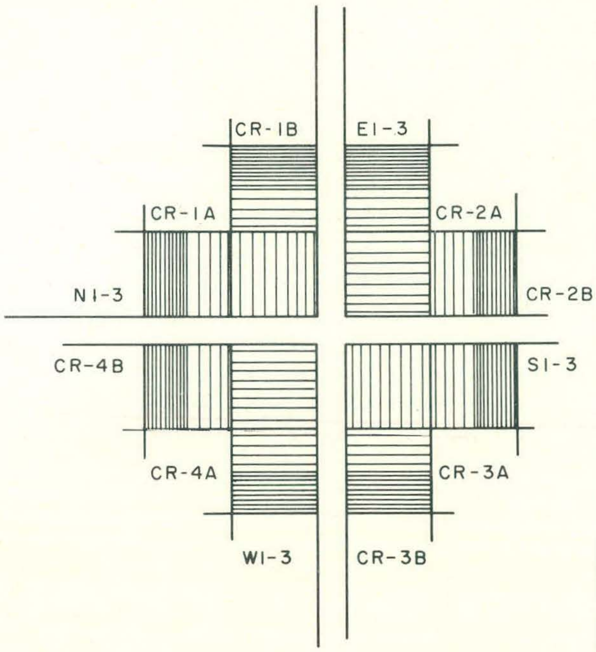

60-3386

Fig. 9 - Details of Central Core Region for Positive Void Coefficient Core

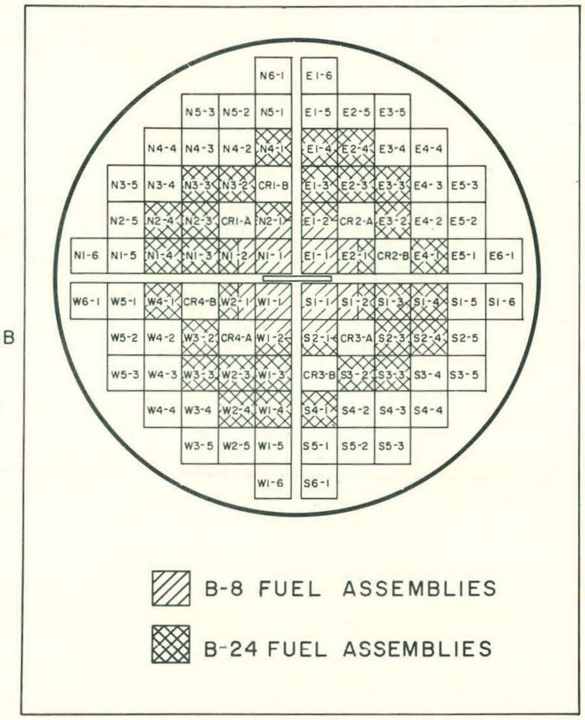

60-3502

Fig. 10 - Spert II Critical Core Configuration for Positive Void Coefficient Core

A preliminary void coefficient measurement was made to determine if the desired objectives had been achieved. This measurement was done with 5 in. x 1 in. x 0.100 in. magnesium strips which were placed in the B-8 fuel assemblies. They were positioned so that the centerline of the strip was at the reactor fuel centerline. With a single strip in each of the B-8 fuel assembly channels a positive void coefficient of approximately 1.9×10^{-2}¢/cm^3 was measured. When single strips were in the channels of only the central four B-8 fuel assemblies a void coefficient of 2.7×10^{-2}¢/cm^3 was measured. A void coefficient of this magnitude and extent is sizeable enough that subsequent transient tests should allow an evaluation of its effect on the safe operation of the system.

IV. SPERT III

A. Measurement of the Neutron Flux Distribution (W. J. Neal and R. W. Garner)

As a part of the power calibration described in Section B, below, and to provide information for future use in the analysis of transient data, the neutron flux distribution has been measured in the Spert III C-19/52 core.* The activation measurement utilized cobalt wires which were irradiated for 10 minutes at a power level of about 270 kw. Wires were placed vertically in the center of each fuel assembly, in the center of one control rod of the south quadrant of the core and in other selected locations of the core and reflector region as shown in Fig. 11. In the figure the crosses indicate positions used for vertical profiles and the dotted lines show where horizontal profiles were obtained. In order to obtain information on the flux profile across an individual assembly, three vertical wires were irradiated in core position S-11, one near the transient rod, one in the center of the assembly, and one away from the transient rod. Data from these three wires were essentially the same.

For the fuel-poison control rod[7] in position S-13 a wire was placed in the center of the assembly extending from the top of the poison section to the bottom of the fuel section. The control rods are provided with flux suppressors in the region between the end of the poison section and the top of the fuel plates as shown in Fig. 12. The portion of the rod labeled point "A" in Fig. 12 is used as a reference point in determining the vertical position of the control rods with respect to the fuel in the core. Fig. 13 shows the effectiveness of the flux suppressors by comparing the shape of the vertical flux profile from the control rod in position S-13 with the vertical profile from the fuel assembly in position S-12.

Representative plots of the vertical profiles for several positions in the core and reflector are shown in Figs. 14, 15 and 16.

As shown in Fig. 11, for the horizontal flux profile three wires were placed in the water channels between fuel assemblies in the following positions: one wire placed horizontally in the water channel between the north and west quadrants from positions W-21 to W-51 at the core horizontal centerline, a second wire in the same horizontal position but at

---

*The notation $L\text{-}N_1/N_2$ core is consistent with that used for all cores tested in Spert reactors. The letter L denotes the type of fuel assembly used; the number N_1 denotes the number of fuel plates per assembly, and N_2 is the number of core lattice positions occupied by both fuel assemblies and the fuel-poison control rods. Hence C-19/52 designates a loading of C-type fuel assemblies having 19 fuel plates per assembly, and a total of 44 fuel assemblies plus 8 control rods in the reactor, i.e., 52 core positions occupied.

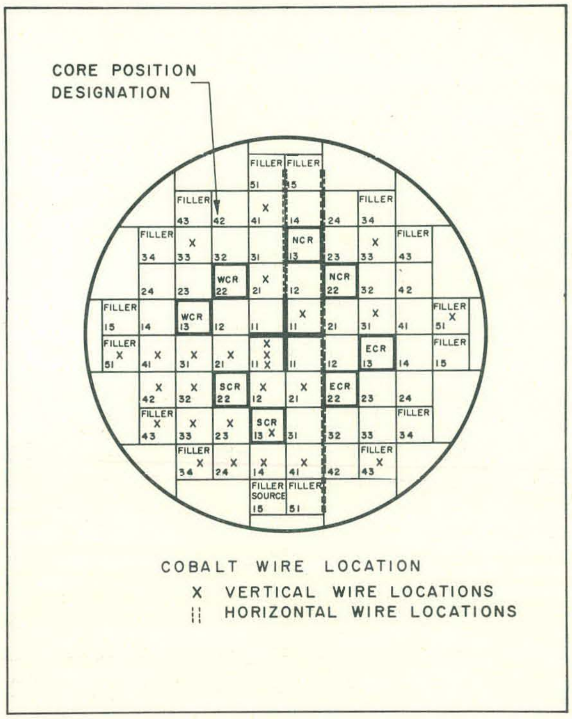

60-3501

Fig. 11 - Location of Flux Monitors in Spert III Core

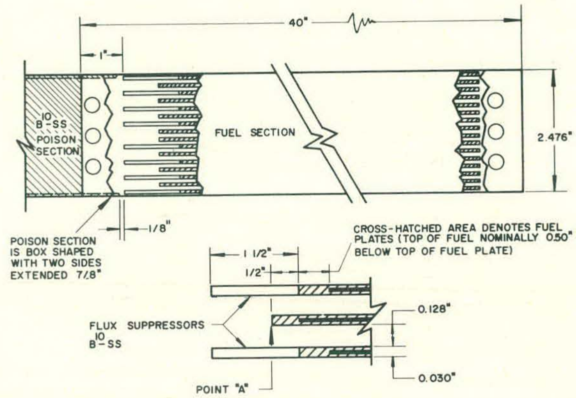

59-5363

Fig. 12 - Details of Flux Suppressor Installation in the Spert III Control Rods

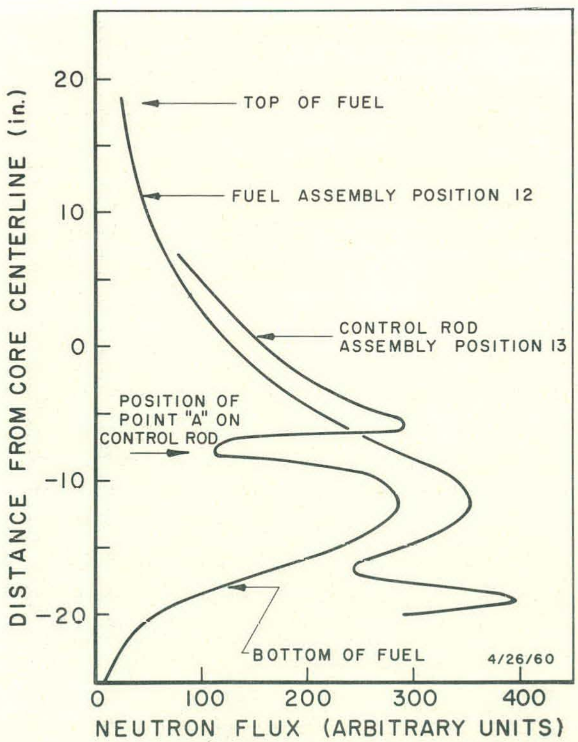

60-3497

Fig. 13 - Spert III Vertical Flux Profile by Cobalt-60 Wires

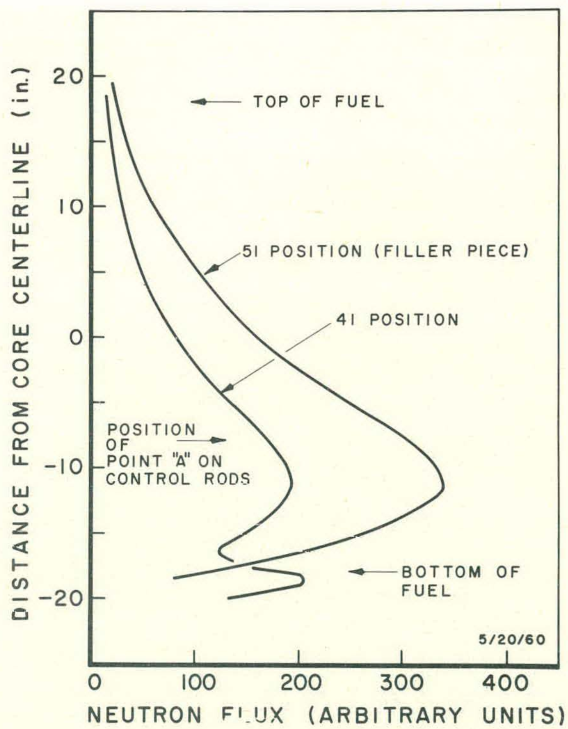

60-3500

Fig. 14 - Spert III Vertical Flux Profile by Cobalt-60 Wires

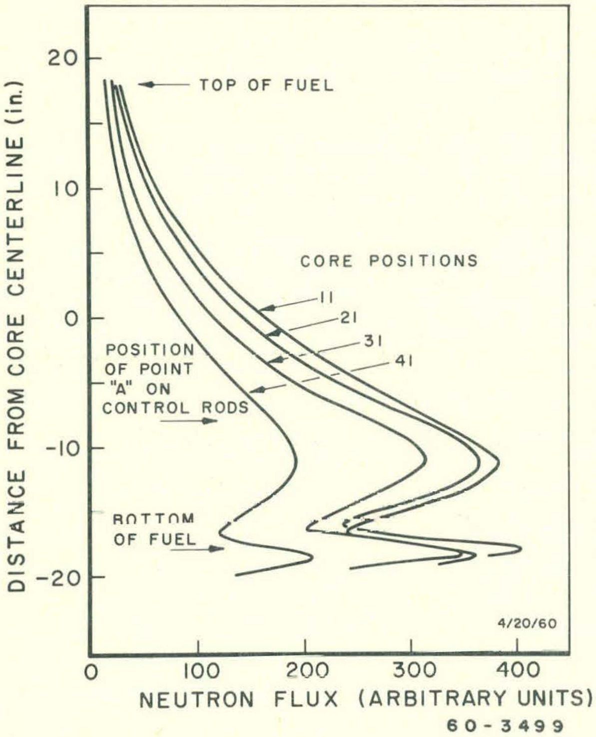

Fig. 15 - Spert III Vertical Flux Profile by Cobalt-60 Wires

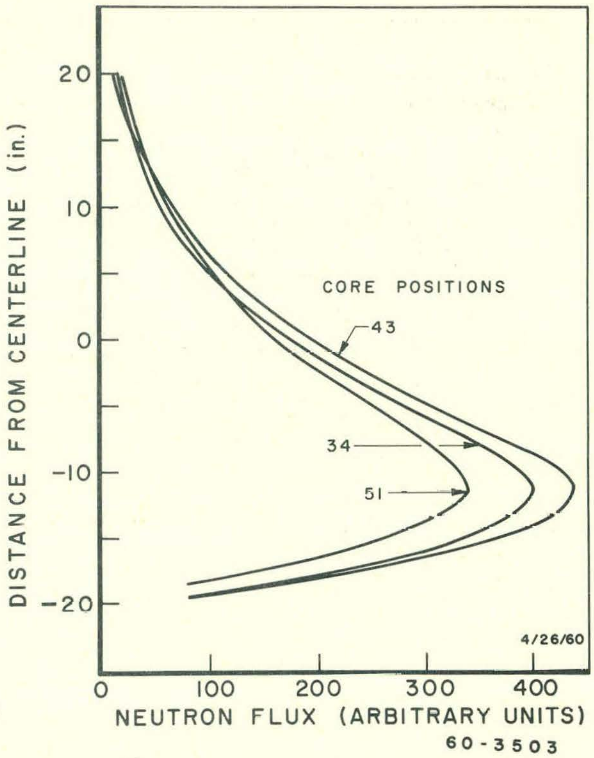

Fig. 16 - Spert III Vertical Flux Profile by Cobalt-60 Wires

the peak of the flux approximately 11-1/2 in. below the core horizontal centerline, and a third wire placed horizontally in the north and east quadrants from E-51 to N-15 at the core horizontal centerline. The horizontal flux profiles are shown in Figs. 17 and 18 for these three wires.

For the Spert III C-19/52 core, the peak to average flux ratio for each fuel assembly position is about 2.1. The ratio of maximum core flux to average core flux is about 2.8. Fig. 19 shows the relative peak and relative average fluxes for the vertical profiles in the south quadrant where the peak flux value of position S-11 has been taken as unity. Average neutron flux (arbitrary units) for the various positions in the core and reflector were determined by integration of the vertical profile for each position over the active core length. For the control rod in position S-13, the average flux was determined by integration only over the 10.25 in. of control rod fuel in the core.

A preliminary flux map had been obtained by the gold foil activation method. The gold foils were placed in the E-21 core position on a plastic foil holder and were irradiated at a power of approximately 33 w for 8 minutes. A comparison was made between the flux profiles obtained from gold foils and Co wire for core position E-21 and is shown in Fig. 20. The excellent agreement in the shape of the flux profiles obtained by the two methods indicates that the differences in the activation cross sections for gold and Co^{59} have no appreciable effect on the shape of the measured flux profile.

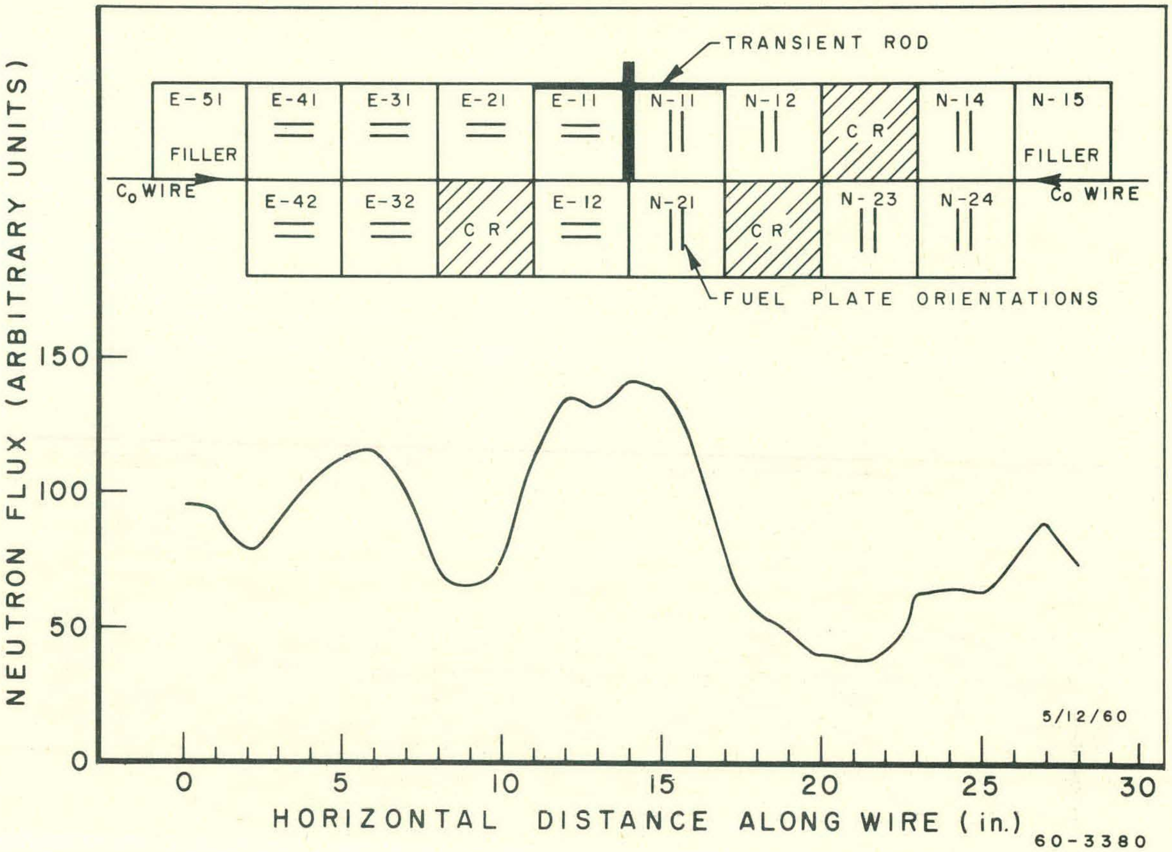

Fig. 17 - Spert III Horizontal Flux Profile by Cobalt-60 Wires

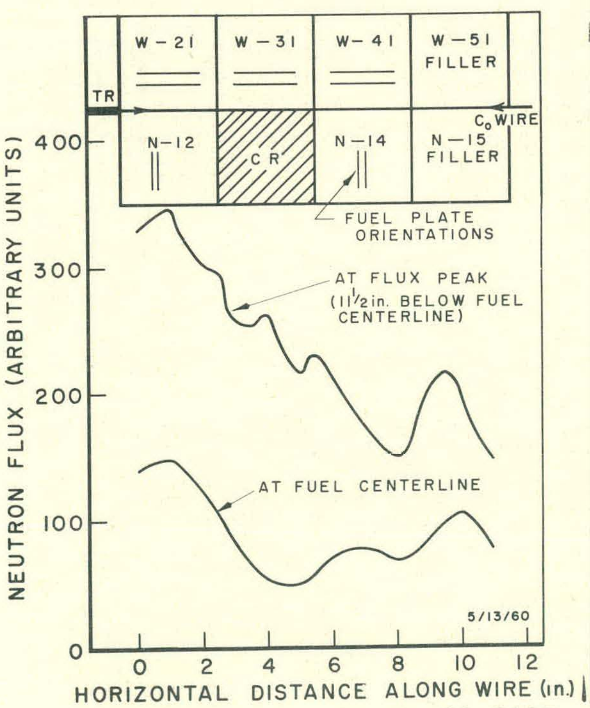

Fig. 18 - Spert III Horizontal Flux Profile by Cobalt-60 Wires

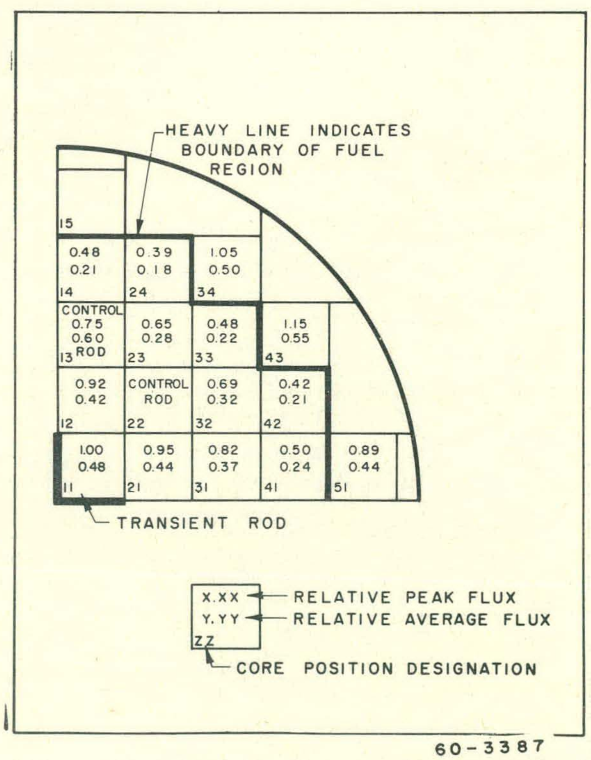

Fig. 19 - One Quadrant of Spert III Core Showing Relative Flux Distribution

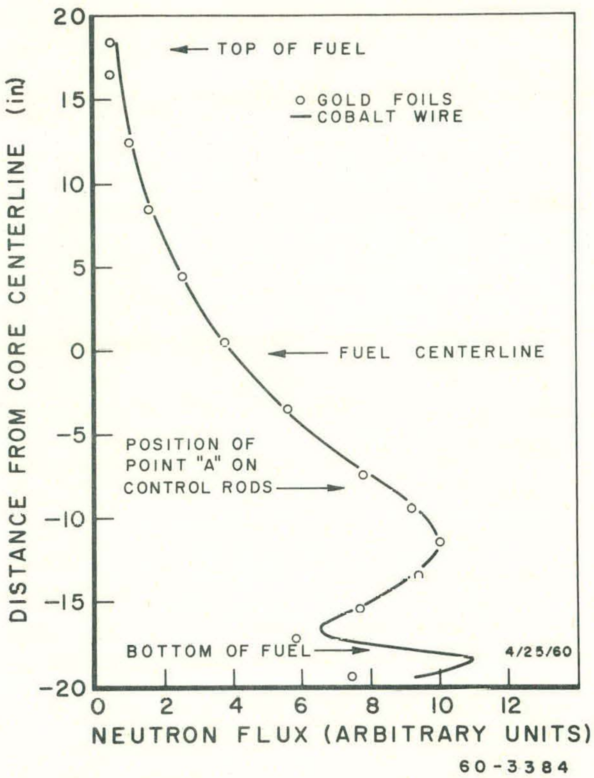

Fig. 20 - Spert III Vertical Flux
Profile Comparing Gold Foil
with Cobalt-60 Wire

B. Power Calibration (C. R. Toole)

The flux distribution data described in the preceding section were used to obtain power calibration factors at ambient temperature for the Spert III neutron chambers used to measure power during transient tests. During irradiation of the cobalt wires at a constant power level, the output of each of the neutron chambers was recorded on an oscillograph. These detectors were mounted in reproducible locations near the reactor. The energy release for the irradiation was calculated from the relationship

$$E = C \bar{\phi} \Sigma_f V$$

where E = the total energy released in watt-sec
C = 2.97×10^{11} watt-sec/fission
$\bar{\phi}$ = the average integrated flux over the core in nvt
Σ_f = the macroscopic fission cross section for the core = 0.11 cm^{-1}
and V = the volume of the core = 2.46×10^5 cm^3.

Segments from three cobalt wires were counted in a calibrated chamber at the MTR, thus providing a conversion factor from count rate to nvt. The wire activation measurements were converted to flux values and the average nvt was obtained. By substituting into the equation, the total energy release for the irradiation and, hence, the average power was calculated. Combining the power level with the current output of the neutron chambers yields an approximate calibration number for each chamber in Mw/μa. The results indicate that powers ranging from 5 w to 20 Gw can be measured under ambient conditions with the present arrangement of four chambers.

V. ENGINEERING

A. Preliminary Hydraulic Investigation of the Type "D" Fuel Assembly (J. F. Koenig)

1. Introduction

The type "D" fuel assembly was designed for use as the initial core of the Spert IV reactor. The primary design consideration was to provide a core whose nuclear and hydraulic characteristics could be readily altered, thereby providing maximum experimental flexibility. The resulting fuel assembly is shown in Fig. 21. A square aluminum tube contains removable fuel plates and removable side plates. The fuel plates are positioned by the side plates and are supported at the bottom by the end box and at the top by a removable hold-down bar.

The Spert IV reactor has been designed for a flow rate of 5000 gpm. An investigation was undertaken to calculate the overall pressure drop of the assembly and to experimentally verify the pressure drop relationship, mechanical integrity and the pressure distribution between water channels across an assembly.

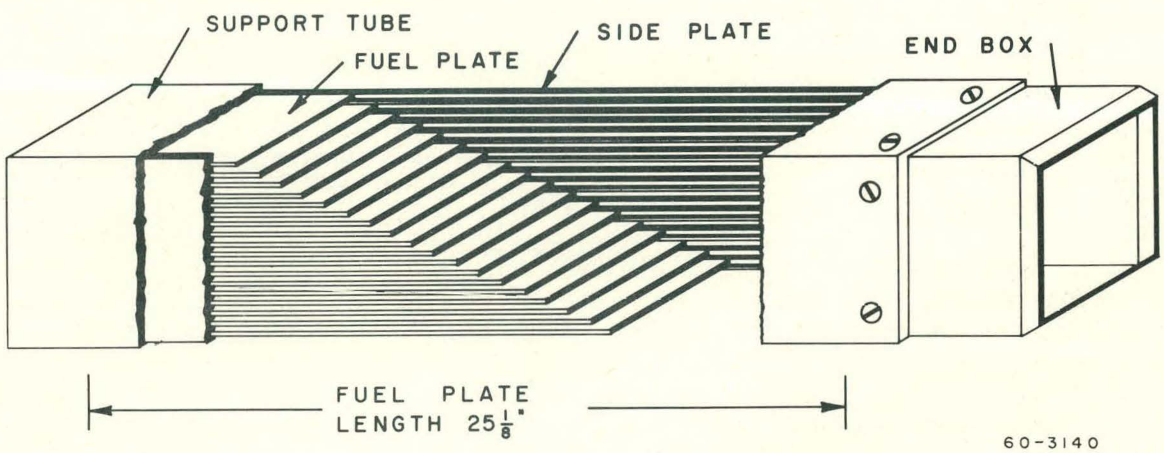

Fig. 21 - Cross Section of the Spert Type "D" Fuel Assembly

2. Calculated Hydraulic Characteristics

The pressure drop versus flow relationship was calculated by using conventional pressure drop techniques. In the calculation, the following assumptions were made:

a) The flow outside of the assembly was neglected.

b) It was assumed that the channel width was the average width, 0.092 in. Since the fuel plates have a 0.013 in. clearance in the retaining slots of the side plates, the channel width may vary from 0.079 in. to 0.105 in. Although the instantaneous channel width may vary from 0.079 to 0.105 in., the pressure drop may be approximated by assuming the average value of 0.092 in.

c) The roughness of the end box, fuel plates, and a support tube is that of drawn tube. Previous calculations on the type "B" element, which agreed with the experimental data, substantiated this assumption.

d) The pressure drop through each channel was the same.

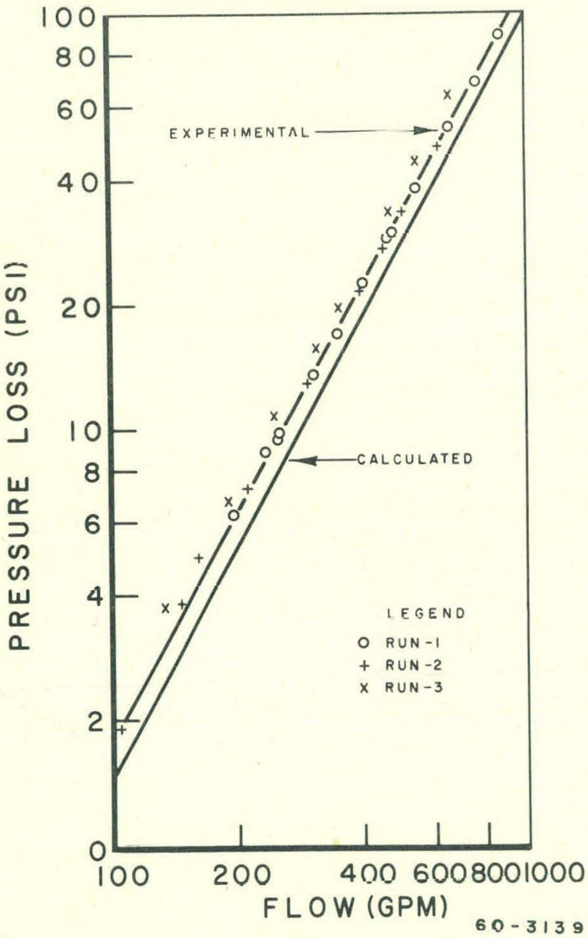

Fig. 22 - Experimental and Calculated Pressure Loss Relationship for the Spert Type "D" 18-Plate Fuel Assembly

The results of the calculations for 1 atm pressure and 85°F are shown in Fig. 22.

3. Description of Apparatus

An experimental test was conducted on the type "D" assembly in the ETR Hydraulic Test Loop in order to verify the calculated overall pressure drop versus flow relationship and to determine the pressure distribution between channels.

A schematic diagram of the hydraulic loop is shown in Fig. 23. The fuel assembly was inserted into the test jig and the flow varied from 130 gpm to 860 gpm in order to obtain hydraulic characteristics over a wide range of flows. In the first series of tests, static pressure points were located in each channel 23-1/2 in. from the bottom of the dummy aluminum fuel plates and the pressure profile was measured. In addition, static pressures were measured at the top and bottom of the fuel assembly from which the overall pressure drop was determined. Observation windows were located in the side plates in order to visually observe the extent of fuel plate vibration. In the second series of tests, the static tubes were removed and the aluminum fuel plates replaced with dummy fuel plates made of Al-U-238 alloy clad with aluminum. Movies were made of the fuel plate vibration for flow rates up to 610 gpm in order to obtain a permanent record. In the third series of tests, static tubes were again attached to aluminum fuel plates and placed in a support tube without observation windows. The pressure taps for this test were

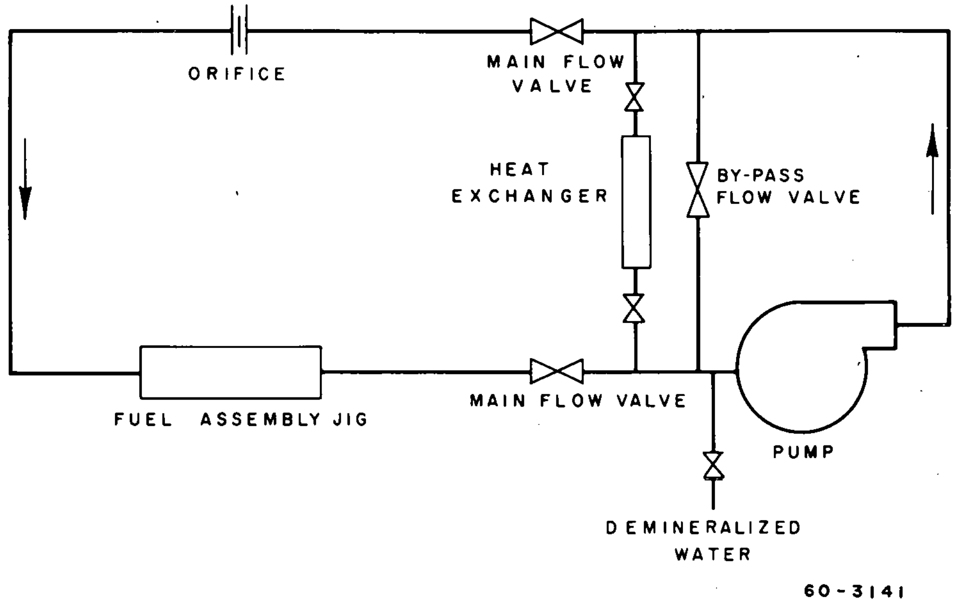

Fig. 23 - Schematic Diagram of the ETR Hydraulic Test Facility

located 12-1/2 in. from the bottom of the plates.

Further tests are planned to obtain static pressures near the bottom of the fuel plate channels and to obtain the flow through each channel.

4. Discussion

In Fig. 22, the overall pressure drop is plotted as a function of flow. The experimental results compare quite closely with the calculated relationship. In Fig. 24 and Fig. 25, the channel pressure profile is plotted for the top and middle of the fuel assembly, respectively. The pressure profile for the top of the assembly is quite flat. This is probably due to the ability of the fuel plates to move axially in the slot, thus equalizing the pressure differences. The pressure profile for the middle of the assembly is much more erratic. This was the reverse of what was expected since the entrance effects would be at a minimum at this point. The variation may be due to velocity effects on the static pressure points.

From Figs. 24 and 25 it can be seen that there is a pressure rise at both sides and the center. The increased pressure in the center of the assembly is probably due to flow restriction caused by the location of the lifting bail. The pressure increase at sides of the assembly is due to the reduced flow rates in the outside channels caused by the drag effects of the support tube walls in conjunction with entrance and exit geometry.

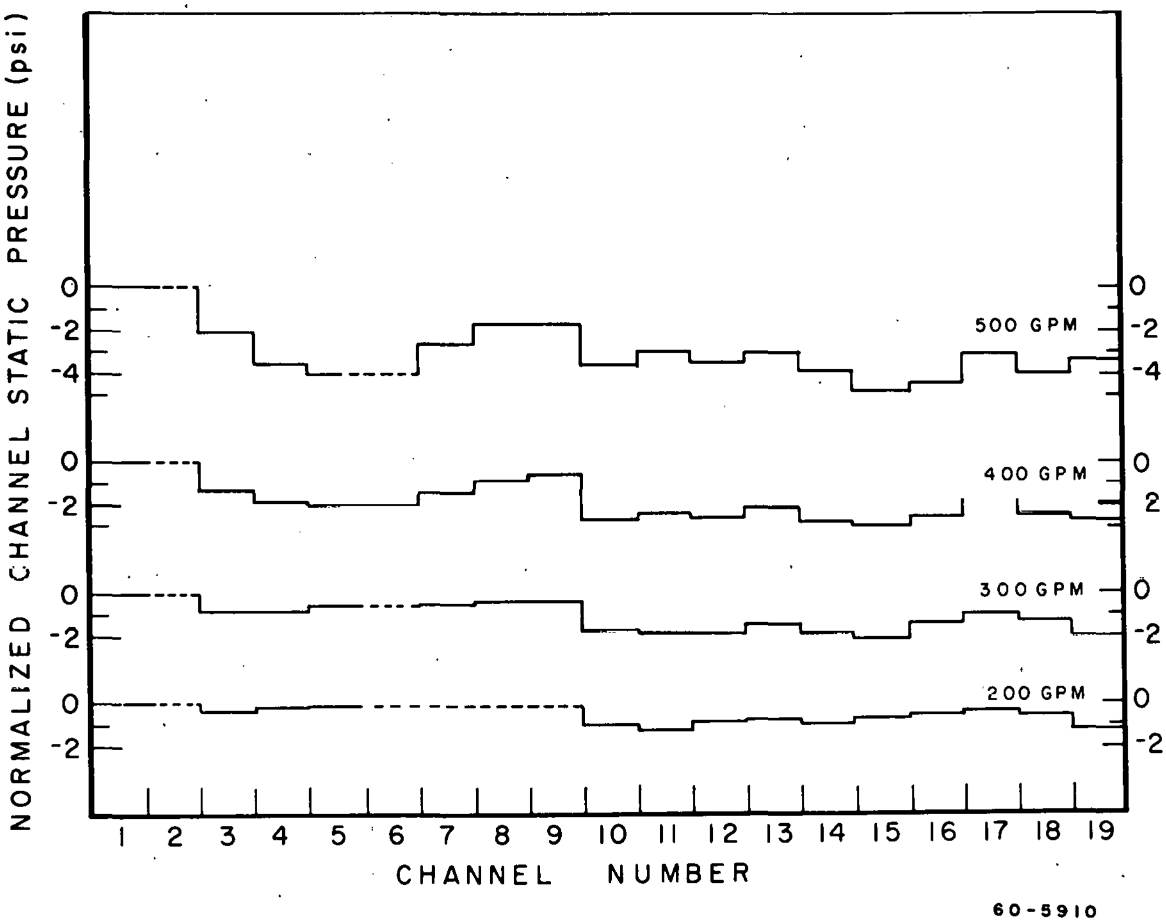

Fig. 24 - Channel Static Pressure Distribution 23-1/2 in. from the Bottom of the Fuel Plate

Study of the motion pictures indicated the following:

a) All the plates vibrated in a random fashion in the slots.

b) The amplitude of plate vibration was not a function of the flow. More quantitative analysis indicated the amplitude of vibration was approximately the same as the channel tolerances, 0.013 in.

c) No bending of the fuel plates could be detected.

It can be concluded that the fuel assembly is acceptable for the design flow rate of the Spert IV reactor, which is about 300 gpm per assembly. However, the flow depression in the center of the assembly should be eliminated by redesign of the lifting bail.

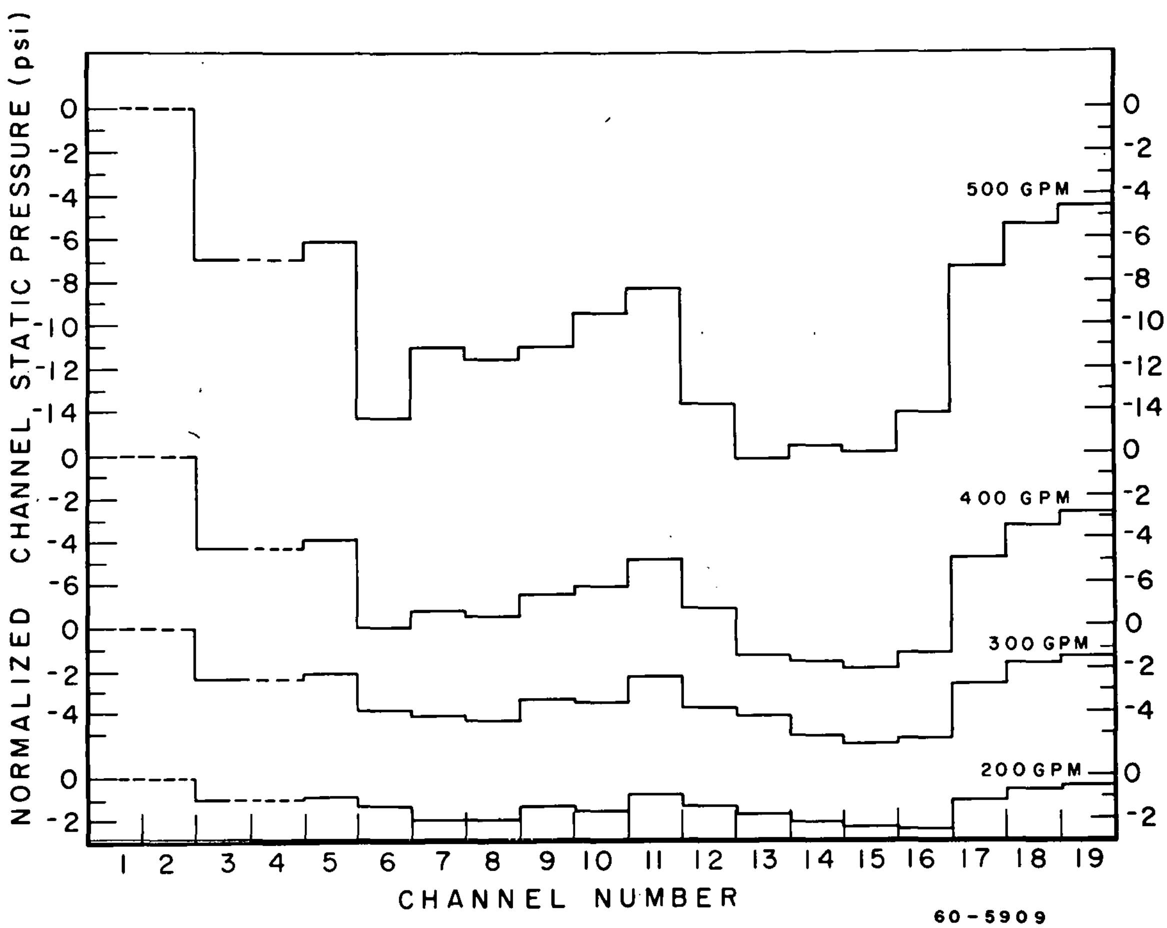

Fig. 25 - Channel Static Pressure Distribution 12-1/2 in. from the Bottom of the Fuel Plate

B. Calculation of the Hydraulic Characteristics of the Type "B" Assembly (J. F. Koenig)

1. Introduction

An investigation was undertaken to calculate the pressure drop versus flow relationship for the type "B" fuel assembly and control rod. This study was desirable since the flow relationship was needed to predict the flow pattern and pressure drop in a core composed of the "B" type assemblies and control rods at elevated temperatures and pressures.

The type "B" fuel assembly is shown in Fig. 26. It is composed of a lower end box extension, a lower end box, a fuel plate section and an upper lifting bail section. The fuel plate section contains the side plates to which four fuel plates are permanently brazed. The side plates have slots that will accommodate an additional 20 plates. The side plate grooves are such that an 8, 12, or 24 plate assembly can be assembled while retaining a uniform channel spacing. Hydraulic calculations were made for each of these configurations at a pressure of 400 psi and temperatures of 100°F, 200°F, 300°F, and 400°F.

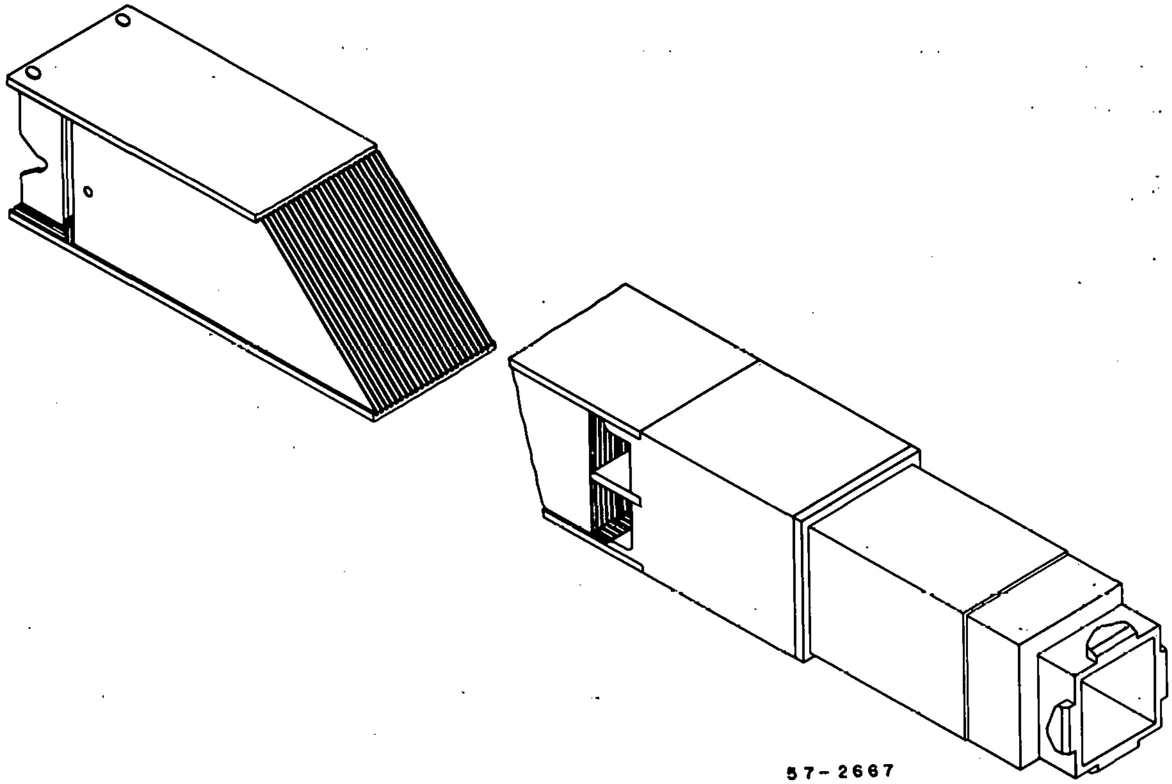

Fig. 26 - Cross Section of the Spert Type "B" Fuel Assembly

The control rods for the Spert II type "B" core are shown in Fig. 27. Each control rod contains a lower end box, a fuel section, a flux suppressor section, and a poison section. The two control rods are connected to a common yoke which is, in turn, connected to the control rod drive unit. The control rods are available with either 5, 12, or 17 fuel plates in the fuel section. Hydraulic calculations were made on each of the configurations at a pressure of 400 psi and temperatures of 100°F, 200°F, 300°F, and 400°F.

2. Method of Calculation

The pressure drop versus flow relationship for each component was derived by standard pressure drop relationships. In the calculations for the fuel assembly the following assumptions were made:

a) There is no flow around the outside of the end box extension. The only flow through the lower grid is caused by the unevenness of the lower grid and fuel assembly end box extension. Since this flow would be small and difficult to accurately predict, it was neglected.

b) The flow on the outside of the side plate section can be neglected. When the flow reaches the fuel plate section, part of the flow may travel along the outside side plate of the assembly. Since this channel dimension is quite small, the calculated pressure drops were quite large for a small flow rate. However, this channel flow was a small part of the total flow (less than 0.5%) and the flow was neglected.

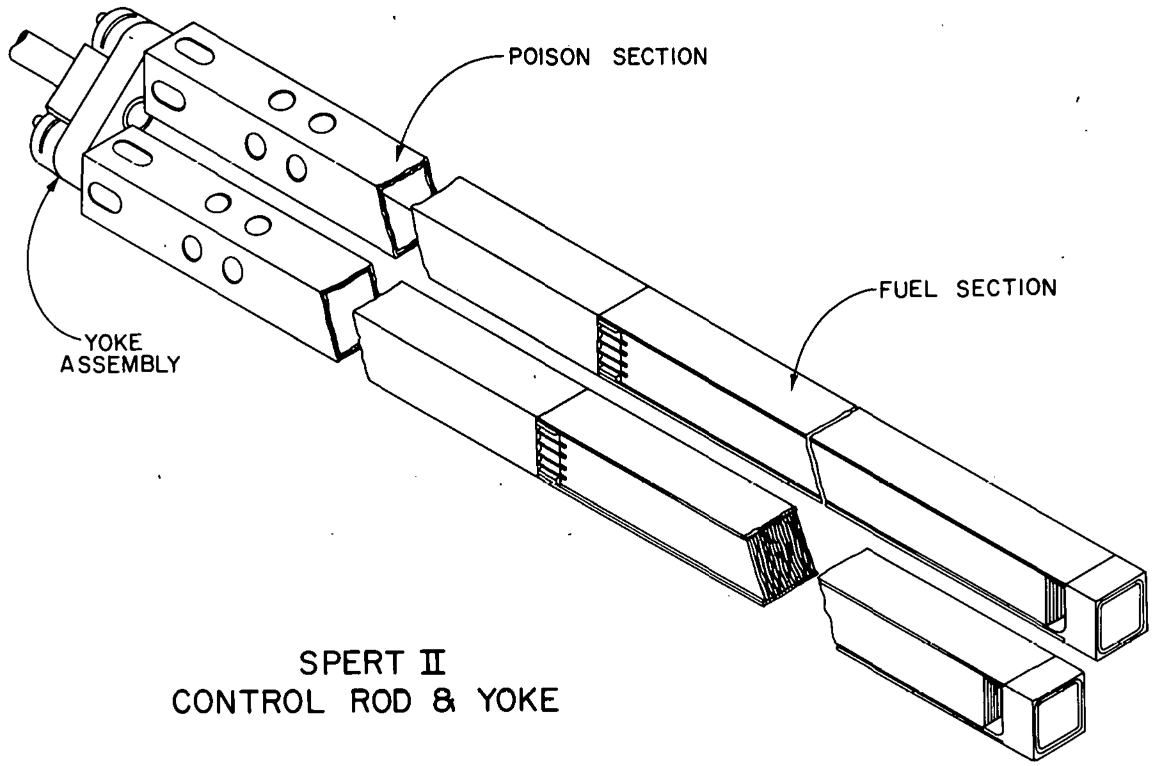

Fig. 27 - Cross Section of the Spert Type "B" Control Rod

c) The pressure drop in each channel of the fuel assembly was assumed to be equal. The previously reported[8] experimental pressure profile at the top of the assembly, which is an indication of the flow distribution, was quite flat. This is probably due to the lack of obstructions in the lower end box and upper end box and the fact that the end boxes were square. Also, any unequal pressure distribution would cause the fuel plates to move in the slot, thus equalizing the channel pressure differences. Therefore, the assumption of equal pressure drops is a valid assumption.

The assumptions made for the control rod calculation are:

a) Flow on the outside of the side plate section was neglected.

b) The pressure drop in each fuel channel was assumed to be the same.

3. Results

The results of the calculation are shown in Fig. 28 for an 8 plate, 12 plate, and 24 plate fuel assembly for 400 psi pressure and temperatures of 100°F, 200°F, 300°F and 400°F. The experimental pressure drop-flow relationship for the 24 plate assembly is plotted for comparison purposes.

The results of the calculation for the 5, 12, and 17 plate control rod are shown in Fig. 29. The calculations were made for a pressure of 400 psi and water temperatures of 100°F, 200°F, 300°F and 400°F.

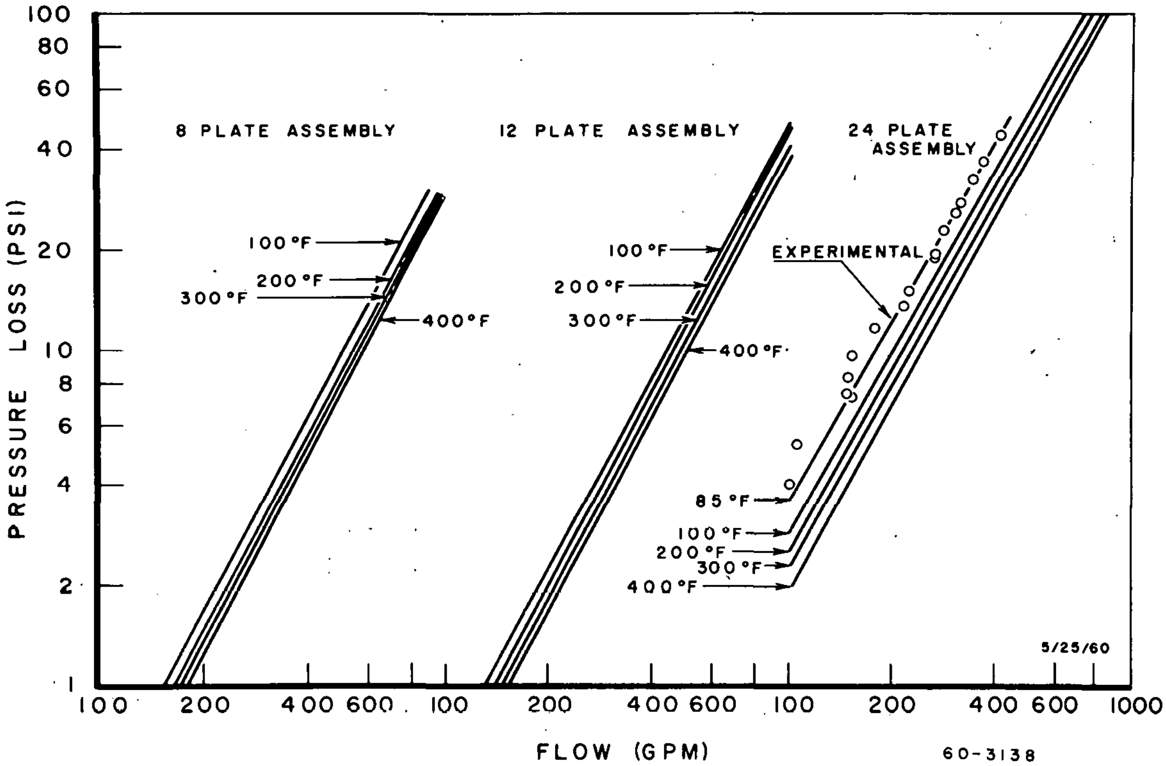

Fig. 28 - Calculated Pressure Loss Relationship for the 8, 12, and 24-Plate Spert Type "B" Fuel Assembly

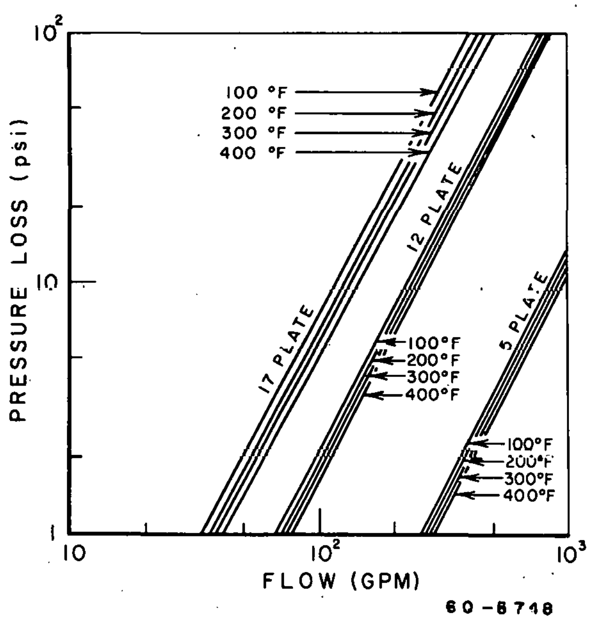

Fig. 29 - Calculated Pressure Loss Relationship for the 5, 12, and 17-Plate Spert Type "B" Control Rod

VI. REFERENCES

1. E. G. Silver and J. Lewin, "Safeguard Report for a Stainless Steel Research Reactor for the BSF (BSR-II)", ORNL-2470 (1958).

2. G. E. Hansen, "Assembly of Fissionable Material in the Presence of a Weak Neutron Source", Nuclear Sci. and Eng., 8, 709 (1960).

3. R. A. Zahn, "Quarterly Progress Report, Reactor Projects Branch", July, August, September, 1957, G. O. Bright, ed., IDO-16416, p. 10, (October 1, 1957).

4. G. F. Brockett, "Quarterly Progress Report, Reactor Projects Branch", April, May, June, 1958, G. O. Bright, ed., IDO-16489, pp. 111-121 (January 19, 1959).

5. K. E. Krauter, "Quarterly Progress Report, Reactor Projects Branch", October, November, December, 1958, F. L. Bentzen, ed., IDO-16537, pp. 65-67 (September 1, 1959).

6. W. E. Nyer, "Quarterly Progress Report, Reactor Projects Branch", January, February, March, 1959, J. A. Norberg, ed., IDO-16539, pp. 48-54 (November 20, 1959).

7. F. Schroeder, W. J. Neal, C. R. Toole and R. A. Zahn, "The Spert III Reactor Nuclear Startup", IDO-16586, pp. 16-17 (March 18, 1960).

8. J. A. Norberg, "Quarterly Progress Report, Reactor Projects Branch", July, August, September, 1957, G. O. Bright, ed., IDO-16416, pp. 63-65 (October 1, 1957).

PHILLIPS
PETROLEUM
COMPANY

ATOMIC ENERGY DIVISION